Piezobiocatalysis

Ultrasound-Driven Enzymatic Oxyfunctionalization of C-H Bonds

Yoon, Jaeho; Kim, Jinhyun; Tieves, Florian; Zhang, Wuyuan; Alcalde, Miguel; Hollmann, Frank; Park, Chan Beum

DOI
10.1021/acscatal.0c00188

Publication date
2020

Document Version
Final published version

Published in
ACS Catalysis

ACS Catalysis

pubs.acs.org/acscatalysis Letter

Piezobiocatalysis: Ultrasound-Driven Enzymatic Oxyfunctionalization of C−H Bonds

Jaeho Yoon, Jinhyun Kim, Florian Tieves, Wuyuan Zhang, Miguel Alcalde, Frank Hollmann,* and Chan Beum Park*

Cite This: *ACS Catal.* 2020, 10, 5236−5242 Read Online

ACCESS | Metrics & More | Article Recommendations | Supporting Information

ABSTRACT: Peroxygenases have long inspired the selective oxyfunctionalization of various aliphatic and aromatic compounds, because of their broad substrate spectrum and simplicity of catalytic mechanism. This study provides a proof-of-concept of piezobiocatalysis by demonstrating peroxygenase-catalyzed oxyfunctionalization reactions fueled by piezocatalytically generated H_2O_2. Bismuth oxychloride (BiOCl) generated H_2O_2 in situ via an oxygen reduction reaction under ultrasonic wave conditions. Through the simple combination of water, ultrasound, recombinant, evolved unspecific peroxygenase from *Agrocybe aegerita* (r*Aae*UPO), and BiOCl, the piezobiocatalytic platform accelerated selective hydroxylation of ethylbenzene to enantiopure (*R*)-1-phenylethanol [total turnover number of r*Aae*UPO ($TTN_{rAaeUPO}$), 2002; turnover frequency, 77.7 min^{-1}; >99% enantiomeric excess (ee)]. The BiOCl−r*Aae*UPO couple also catalyzed other representative substrates (e.g., propylbenzene, 1-chloro-4-ethylbenzene, cyclohexane, and *cis*-*β*-methylstyrene) with high turnover frequency and selectivity. We alleviated the oxidative stress of piezocatalytically generated $OH^{\bullet}$ on r*Aae*UPO by spatial separation of r*Aae*UPO and BiOCl, which resulted in greatly enhanced $TTN_{rAaeUPO}$ of >3900 and the notable prolongation of reaction time. Overall, the BiOCl−r*Aae*UPO couple serves as a mechanical-to-chemical energy conversion platform for driving peroxygenase-catalyzed reactions under ultrasonic conditions.

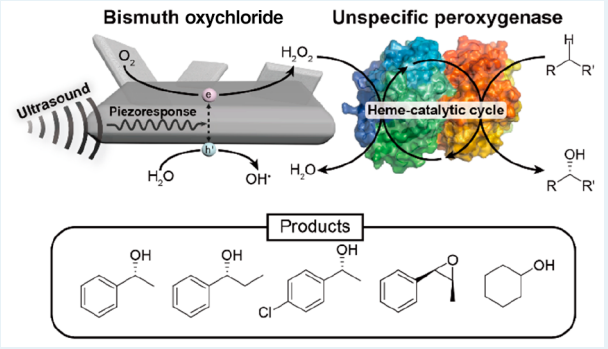

KEYWORDS: *oxidation, oxyfunctionalization, peroxygenase, piezocatalysis, piezobiocatalysis*

INTRODUCTION

Peroxygenases (unspecific peroxygenase, UPO, IUBMB classification: EC 1.11.2.1) are highly versatile heme-containing enzymes for the selective oxyfunctionalization of inert C−H bonds or C=C bonds.[1,2] Recently, UPOs have attracted enormous interest as catalysts, because of their broad substrate spectra and high selectivity (e.g., chemoselectivity, regioselectivity, and enantioselectivity).[3,4] Unlike the cytochrome P450 monooxygenases that are dependent on complex electron transport pathways, peroxygenases use hydrogen peroxide (H_2O_2) as an oxygen donor to generate the catalytically active oxyferryl-heme species (Compound I). The simplicity of the catalytic mechanism makes peroxygenases unrestrained to O_2-induced unwanted side reactions.[5] Despite this fascinating feature, practical application of peroxygenases is often hindered by a rapid inactivation of the enzyme at high concentrations of H_2O_2;[2,6] therefore, effectively controlled in situ generation of H_2O_2 is essential for efficient and robust peroxygenase catalysis. To date, various methods (e.g., chemical,[7] enzymatic,[4,8] photochemical,[9,10] electrochemical,[11] and photoelectrochemical[12]) have been reported for in situ provision of H_2O_2.

However, most of the above-mentioned H_2O_2-generation methods imply the reductive activation of molecular oxygen using sacrificial electron donors, which complicates the reaction schemes. Water would be ideal as a sacrificial electron donor, because it serves as a solvent for most peroxygenase reactions. Moving beyond the conventional approaches, herein, we report on a new concept, termed "piezobiocatalysis", by employing piezocatalytic property of bismuth oxychloride (BiOCl) to unceasingly provide H_2O_2 for biocatalytic oxyfunctionalization reactions (Scheme 1). Piezoelectric materials have long been studied for a wide range of applications (e.g., sensors, actuators, and energy harvesters), because of their reversible mechanical-to-electrical energy conversion property.[13−15] Furthermore, increasing studies on direct mechanical-to-chemical energy conversion—termed

Received: January 12, 2020
Revised: March 9, 2020
Published: March 18, 2020

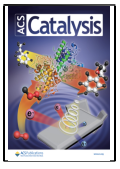

https://dx.doi.org/10.1021/acscatal.0c00188
ACS Catal. 2020, 10, 5236−5242

Scheme 1. Schematic Illustration of Piezobiocatalytic Oxyfunctionalization Reactions by BiOCl−r*Aae*UPO Hybrid[a]

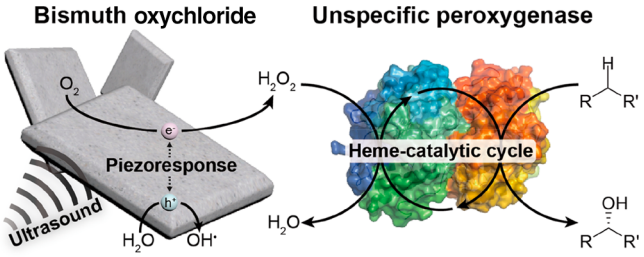

[a]Piezoelectric BiOCl microsheets induce piezocatalytic reduction of O_2 to H_2O_2 under ultrasonic irradiation. The in-situ-generated H_2O_2 activates the redox center of an unspecific peroxygenase to catalyze selective oxyfunctionalization of various organic compounds.

piezocatalysis or the piezoelectrochemical process—have been reported;[16−18] piezocatalysis is an approach for driving redox reactions (e.g., H_2 evolution, pollutant degradation) using free charge carriers generated by piezo-response.[19−21] BiOCl is a V−VI−VII ternary semiconductor material that exhibits anisotropic ferroelectric properties.[22,23] The unique layered structure consists of stacked $[Bi_2O_2]^{2+}$, and Cl^- slabs induce internal electric fields perpendicular to the $[Bi_2O_2]$ slabs, facilitating efficient charge separation along the [001] direction.[24,25] A recent report substantiated a piezocatalytic oxygen reduction reaction by BiOCl through the conversion of applied stress (e.g., ultrasound) into chemical energy in the form of H_2O_2.[26] The in situ supply of H_2O_2 without the need for additional catalysts is an attractive approach for steadily fueling peroxygenase catalysis and minimizing unwanted side reactions and the amassing of valueless byproducts. To demonstrate piezobiocatalysis, we employed BiOCl microsheets to drive peroxygenase-catalyzed selective oxyfunctionalization reactions (e.g., hydroxylation and epoxidation).

RESULTS AND DISCUSSION

We prepared single-crystalline BiOCl microsheets via a one-pot hydrothermal process (180 °C, 24 h) of $Bi(NO_3)_3$ and KCl.[24] Our analyses, using scanning electron microscopy and transmission electron microscopy (TEM), showed sheet-shaped BiOCl crystals with a width of 1−3 μm and a thickness of 200−500 nm (see Figure 1A, as well as Figure S1 in the Supporting Information). The powder X-ray diffraction (XRD) diffractogram (Figure S2 in the Supporting Information), selected-area electron diffraction (SAED) pattern (Figure 1B),

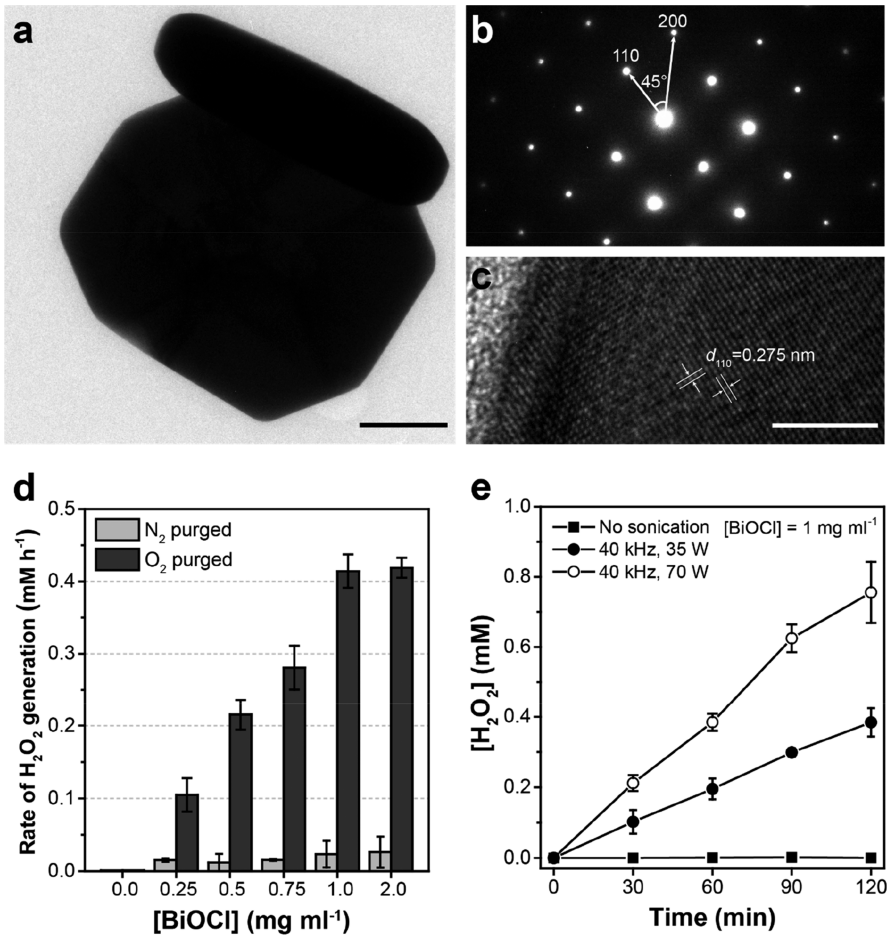

Figure 1. (A) Transmission electron microscopy (TEM) image. Scale bar = 500 nm. (B) Selected-area electron diffraction pattern. (C) High-resolution TEM image. Scale bar = 5 nm. (D) Rate of H_2O_2 generation with increasing concentration of BiOCl. Reaction conditions: BiOCl in a N_2- or O_2-purged Tris buffer (50 mM, pH 7.0) under ultrasonic irradiation (40 kHz, 70 W). (E) Dependency of H_2O_2 generation on the power of ultrasonic wave. Reaction conditions: 1.0 mg mL^{-1} BiOCl in an O_2-purged Tris buffer (50 mM, pH 7.0). All reported values represent mean ± standard deviation (SD) values (n = 3).

https://dx.doi.org/10.1021/acscatal.0c00188
ACS Catal. 2020, 10, 5236−5242

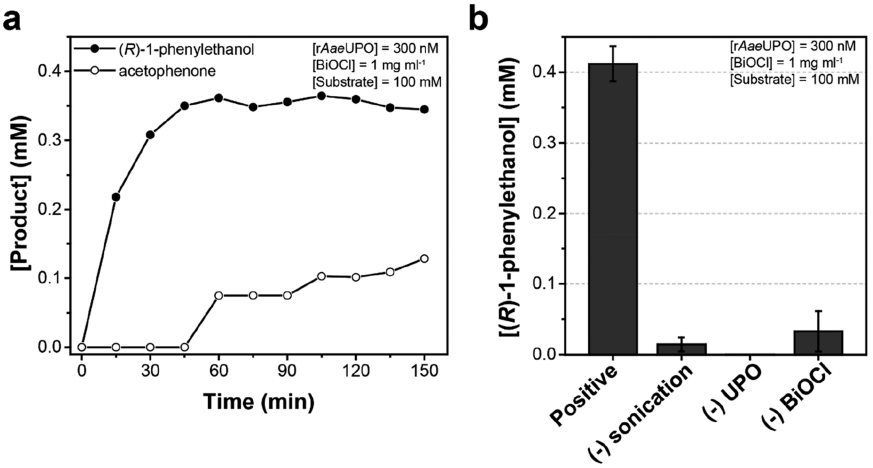

Figure 2. Piezobiocatalytic oxyfunctionalization of ethylbenzene. (A) Piezobiocatalytic production of (*R*)-1-phenylethyanol and acetophenone for 2 h. (B) A series of control experiments for each component (i.e., BiOCl, r*Aae*UPO, and sonication). Reaction conditions: 1 mg mL^{-1} BiOCl; 300 nM r*Aae*UPO; 100 mM ethylbenzene; applied ultrasound (40 kHz, 70 W); solvent: an O_2-purged Tris buffer (50 mM, pH 7.0).

and high-resolution TEM (HRTEM) image (Figure 1C) were consistent with the literature,[24,27] further indicating the high purity and crystallinity of the samples with highly exposed {001} facets. We examined the chemical states and surface composition of BiOCl sheets using X-ray photoelectron spectroscopy (XPS), which revealed the clear indices of binding energy peaks to the characteristic peaks of Bi^{3+}, O^{2-}, and Cl^- (see Figure S3 in the Supporting Information); the absence of a peak at ca. 531 eV indicates the lack of surface OH^- on the BiOCl samples.[28,29] The atomic ratio of Bi−O−Cl was ∼1:0.8:1, according to the quantitative XPS. All the data were in agreement with the theoretical and literature values.

We investigated the capacity of BiOCl microsheets to piezoelectrically generate H_2O_2 by exposing a homogeneously suspended BiOCl solution (1 mg mL^{-1}) to ultrasonic wave (40 kHz, 70 W). As shown in Figure 1D, we observed in situ generation of H_2O_2 with a maximum rate of 0.42 mM h^{-1} (using 1 mg mL^{-1} of BiOCl) in an O_2-enriched environment, whereas a negligible amount of H_2O_2 (<0.02 mM h^{-1}) was produced under N_2-rich conditions. The maximum rate of H_2O_2 formation is higher than other reports[30,31] on piezocatalytic H_2O_2 production (0.1 and 0.3 mM h^{-1}). Furthermore, the linear relationship between the amount of generated H_2O_2 and the amplitude of the ultrasound wave is consistent with the literature,[26] verifying the key role of ultrasound energy (Figure 1E). A series of analyses using radical scavengers (e.g., isopropanol as an $OH^•$ scavenger,[32] and benzoquinone as an $O_2^{•-}$ scavenger[33]) confirmed the pathway of H_2O_2 production via O_2 reduction as reported (see Figure S4 in the Supporting Information). Note that H_2O_2 remained stable under ultrasonic irradiation (40 kHz, 70 W) for 3 h (see Figure S5 in the Supporting Information).

Building on the unceasing H_2O_2 generation by BiOCl nanosheets without noticeable decay, we attempted piezobiocatalysis by coupling piezocatalysis with peroxygenase-driven oxyfunctionalization reactions. As a model enzyme, we chose the recombinant, evolved unspecific peroxygenase from *Agrocybe aegerita* (r*Aae*UPO), because of its versatility and promising catalytic activities.[34,35] As displayed in Figure 2A, the BiOCl−r*Aae*UPO system catalyzed the hydroxylation of ethylbenzene under ultrasonic irradiation (40 kHz, 70 W) for 2 h, yielding enantiopure (*R*)-1-phenylethanol [>99% enantiomeric excess (ee)] with an initial conversion rate of 0.87 mM h^{-1} and a total turnover number ($TTN_{rAaeUPO}$) of 1215. In addition, 0.13 mM of acetophenone was produced through r*Aae*UPO-catalyzed oxidation of (*R*)-1-phenylethanol. Note that the initial conversion rate (0.87 mM h^{-1}; see Figure 2A) was higher than H_2O_2 production rate (0.42 mM h^{-1}; see Figure 1D). We attribute it to the increase in H_2O_2 formation rate from 0.42 mM h^{-1} to 0.86 mM h^{-1} in the presence of ethylbenzene (see Figure S6 in the Supporting Information); ethylbenzene functions as an $OH^•$ scavenger,[36,37] which boosts the kinetics of O_2 reduction to H_2O_2. We also conducted a series of control experiments to verify the indispensability of each reaction component (i.e., BiOCl, sonication, and r*Aae*UPO) for piezobiocatalysis. As displayed in Figure 2B, the experimental group produced (*R*)-1-phenylethanol of 0.41 ± 0.03 mM with excellent enantiospecificity (>99% ee), whereas little to no (<0.03 mM) product was detected in the absence of any single component, indicating that the BiOCl−r*Aae*UPO system functions well as an ultrasound-induced biocatalytic platform for chiral oxidation of ethylbenzene.

To elucidate the limiting factors for piezobiocatalytic reactions, we examined biocatalytic performances with respect to the concentrations of r*Aae*UPO and BiOCl. Table S2 in the Supporting Information shows that the overall reaction rate was significantly affected by enzyme concentration. The initial conversion rate of ethylbenzene to (*R*)-1-phenylethanol and the total amount of product were linearly proportional up to an enzyme concentration of 300 nM with an average 0.91 ± 0.27 mM h^{-1} and a maxima of 0.49 mM, respectively. In contrast, the piezobiocatalytic reaction was affected nonlinearly by the concentration of BiOCl (0.2−1.0 mg mL^{-1}), producing 0.27 ± 0.03 mM of (*R*)-1-phenylethanol (>99% ee), on average. The product concentration increased to a maximum of 0.308 mM in proportion to the BiOCl concentration (<0.6 mg mL^{-1}), but decreased at a higher BiOCl concentration (>0.8 mg mL^{-1}). The results imply a possible inhibitory effect of BiOCl on peroxygenase-driven catalysis, which will be discussed later in this paper.

We assessed the piezobiocatalytic platform's applicability to other oxyfunctionalization reactions, such as stereoselective benzylic hydroxylation, alkane hydroxylation, and styrene epoxidation. As summarized in Table 1, r*Aae*UPO successfully

https://dx.doi.org/10.1021/acscatal.0c00188
ACS Catal. 2020, 10, 5236−5242

Table 1. Substrate Scope of Piezobiocatalytic Hydroxylation Reactions[a]

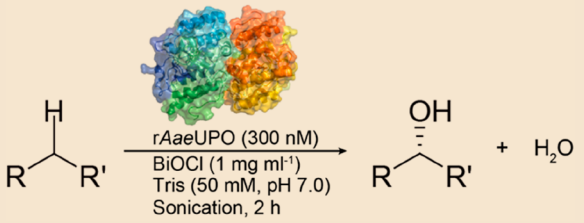

Substrate	Product concentration (mM)	$TTN_{rAaeUPO}$	Initial reaction rate (μM min^{-1})	$TOF_{rAaeUPO}$ (min^{-1})	*ee* (%)
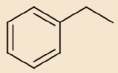	0.601	2002.0	23.3	77.7	>99
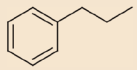	0.121	402.3	3.6	12.0	>99
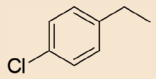	0.417	1389.6	23.8	79.5	71.4
	0.423	1410.5	28.2	94.0	N/A
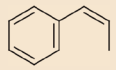	0.215	716.4	14.3	47.5	>99

[a]All quantities were determined from gas chromatographic analyses. Initial reaction rate and TOF were determined at 15 min of reaction. Reaction conditions: 1 mg mL^{-1} BiOCl, 300 nM r*Aae*UPO, and 100 mM substrate ([1-chloro-4-ethylbenzene] = 10 mM) in an O_2-purged Tris buffer (50 mM, pH 7.0) under ultrasonic irradiation (40 kHz, 70 W, 2 h). N/A = not applicable.

catalyzed hydroxylation of propylbenzene ($TTN_{rAaeUPO}$ of 402, >99% ee), 1-chloro-4-ethylbenzene ($TTN_{rAaeUPO}$ of 1390, 71% ee), cyclohexane ($TTN_{rAaeUPO}$ of 1410), and the epoxidation of *cis*-*β*-methylstyrene ($TTN_{rAaeUPO}$ of 720, >99% ee) for 2-h reactions with only trace amounts of overoxidized products. The conversion of ethylbenzene showed the highest $TTN_{rAaeUPO}$ of >2000 (>99% ee) and yield (0.6 mM).

Despite the successful piezobiocatalytic reactions, we observed an undesired cessation of substrate conversion after 2 h (Figure 2A). To address this issue, we examined two potential causes that might hamper long-term operation of the piezobiocatalytic reactions: (1) ultrasound-induced denaturation of the enzyme and (2) reactive oxygen species (ROS)-induced inactivation of the enzyme. To examine possible damage to the r*Aae*UPO by the ultrasonic wave itself, we performed a series of peroxygenase-activity assays on oxidation of 2,2′-azino-bis(3-ethylbenzthiazoline-6-sulfonic acid) under continuous irradiation of ultrasound wave (40 kHz, 70 W) to the enzyme solution for 2 h. As shown in Figure S7 in the Supporting Information, the residual activity remained 100% after ultrasonic treatment. Furthermore, BiOCl did not deactivate r*Aae*UPO in the absence of ultrasound. The results suggest that neither BiOCl nor ultrasound deteriorates the activity of r*Aae*UPO.

In stark contrast, r*Aae*UPO suffered a severe loss of catalytic ability (residual activity: ∼10% after 2 h) in the presence of BiOCl under ultrasonic irradiation (Figure S7), which implies that the piezoresponse of BiOCl plays a critical role in enzyme inactivation. During piezocatalytic O_2 reduction, BiOCl generates free charge carriers (e.g., electrons and holes) under ultrasonic irradiation.[26] The electrons and holes react with O_2 and H_2O, generating superoxide ($O_2^{\bullet-}$) and hydroxyl radical intermediates ($OH^{\bullet}$), respectively, as illustrated in Figure S8 in the Supporting Information. We found a linear relationship between the ROS generation rate and BiOCl concentration (0.25 to 2.0 mg mL^{-1}) (see Figure 3, as well as Figure S9 in the Supporting Information). According to the literature,[10,38] $OH^{\bullet}$ severely impedes peroxygenase-driven catalysis, damaging r*Aae*UPO. Based on the established observations, we hypothesized that piezocatalytically generated ROS (especially $OH^{\bullet}$) may inactivate r*Aae*UPO. To investigate the effect of ROS on r*Aae*UPO's activity, we used radical scavengers, such as superoxide dismutase (SOD, $O_2^{\bullet-}$ scavenger) and isopropanol (IPA, $OH^{\bullet}$ scavenger). We found that the addition of SOD to the BiOCl−r*Aae*UPO system did not improve the reaction performance (see Figure S10 in the Supporting Information), suggesting negligible oxidative stress of $O_2^{\bullet-}$ on the enzyme. In contrast, enzyme activity assays with varying IPA concentration (0−20 mM) showed that the residual activity of r*Aae*UPO improved by a factor of ∼4 with the addition of IPA (see Figure S11 in the Supporting Information), indicating the major role of $OH^{\bullet}$ (rather than $O_2^{\bullet-}$) in the inactivation of r*Aae*UPO.

https://dx.doi.org/10.1021/acscatal.0c00188
ACS Catal. 2020, 10, 5236−5242

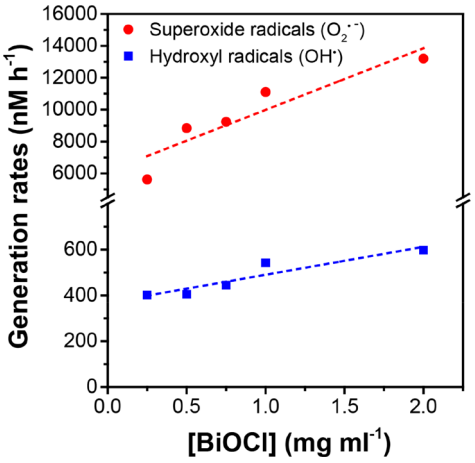

Figure 3. Generation of reactive oxygen species (ROS) by BiOCl-induced piezocatalysis. Superoxide ($O_2^{\bullet-}$) and hydroxyl radicals ($OH^{\bullet}$) were quantified using nitro blue tetrazolium (NBT) and terephthalic acid (TA) assays, respectively. Reaction conditions: BiOCl and assay reagent (NBT or TA) in an O_2-purged Tris buffer (50 mM, pH 7.0) under 1 h of ultrasonic irradiation (40 kHz, 70 W).

Considering the nanosecond-scale half-life[39] and nanometer-scale diffusion distance[40] of $OH^{\bullet}$, we spatially separated BiOCl and r*Aae*UPO to mitigate the negative influence of $OH^{\bullet}$ and accomplish long-term robust piezobiocatalysis. We placed r*Aae*UPO in a dialysis membrane bag with an appropriate pore size (molecular mass cutoff = 14 kDa), which allowed the transport of H_2O_2, substrates, and products through the membrane and minimized direct contact between r*Aae*UPO (51.1 kDa)[35] and BiOCl—thereby attenuating the oxidative stress of short-lived $OH^{\bullet}$. We found that the dialysis membrane did not hinder the generation of H_2O_2, and H_2O_2 concentration was almost similar inside and outside of the membrane (see Figure S12 in the Supporting Information). Surprisingly, the membrane-protected r*Aae*UPO exhibited a significantly improved catalytic performance without any noticeable saturation behavior for 8 h; the product concentration (1.19 mM) and $TTN_{rAaeUPO}$ (3982) were ~3 times higher than those of the free enzyme (see Figure 4). The

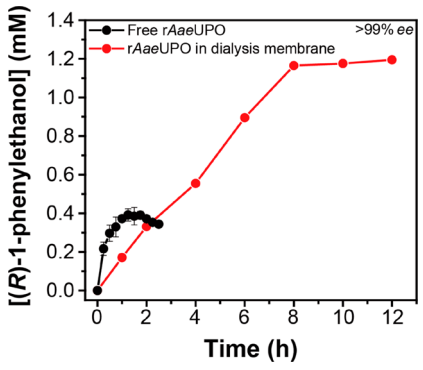

Figure 4. Influence of spatial separation between BiOCl and r*Aae*UPO on piezobiocatalytic hydroxylation of ethylbenzene to (*R*)-1-phenylethanol. Reaction conditions: 1 mg mL^{-1} BiOCl; 300 nM r*Aae*UPO; 100 mM ethylbenzene; applied ultrasound (40 kHz, 70 W); solvent: an O_2-purged Tris buffer (50 mM, pH 7.0). Note that we used a dialysis membrane cellulose (molecular mass cutoff = 14 kDa) to separate BiOCl from r*Aae*UPO. All reported values represent mean ± SD values (n = 3).

decrease of the initial reaction rate (2.85 μM min^{-1}) is ascribed to the diffusion step of substrate through the membrane. The residual activity of the membrane-protected enzyme decreased to ~0.1% after 8 h of piezobiocatalysis (see Figure S13 in the Supporting Information). We attribute the result to the loss of the protection function of the membrane by in-situ-produced radicals; according to the literature,[41] hydroxyl radicals degrade cellulose acetate-based membranes.

Admittedly, the BiOCl–r*Aae*UPO piezobiocatalytic system falls short of the productivities of H_2O_2 formation and UPO catalysis; TTN_{UPO} is more than 10 times lower, compared to that observed for other H_2O_2-generation methods.[4,42] The future efforts will focus on enhancing the efficiency of piezocatalysis and improving the robustness of membranes. For example, the augmentation of the piezocatalyst's internal polarization through crystal structure modification[43] or elemental doping[20] can accelerate the piezocatalytic reaction. In addition, the functionalization of a membrane with sulfates[44] or sulfonates[45] may enhance its chemical stability against oxidative stress by radicals, which elongates the piezobiocatalytic reaction.

CONCLUSIONS

This study provides a proof-of-concept of piezobiocatalysis for the first time. The piezocatalytic system drives peroxygenase reactions in a much simpler way than other existing methods by using a new form of energy (i.e., mechanical energy). The piezobiocatalytic platform has significant advantages over conventional approaches for driving peroxygenase reactions. For example, the use of O_2 is more atom-efficient, compared with glucose oxidase-driven methods using glucose. In contrast to UV light-induced photochemical methods, the UV-induced damage of enzymes can be minimized. Unlike (photo)-electrochemical routes, an additional co-catalyst is not required. Furthermore, the use of water as a solvent and electron donor makes piezobiocatalysis much greener than typical photochemical approaches using organic electron donors (e.g., triethanolamine).[46−48] There is room for further engineering studies (e.g., replenishment of volatile substrates, the introduction of an organic–aqueous two-phase system), which should improve the reaction performance of the BiOCl–r*Aae*UPO couple.

ASSOCIATED CONTENT

Supporting Information

The Supporting Information is available free of charge at https://pubs.acs.org/doi/10.1021/acscatal.0c00188.

Experimental procedures, additional figures, tables for catalyst preparation, catalyst characterization, product analysis (PDF)

AUTHOR INFORMATION

Corresponding Authors

Chan Beum Park − *Department of Materials Science and Engineering, Korea Advanced Institute of Science and Technology (KAIST), Daejeon 305-701, Republic of Korea;* orcid.org/0000-0002-0767-8629; Email: parkcb@kaist.ac.kr

Frank Hollmann − *Department of Biotechnology, Delft University of Technology, Delft 2629 HZ, The Netherlands;* orcid.org/0000-0003-4821-756X; Email: f.hollmann@tudelft.nl

https://dx.doi.org/10.1021/acscatal.0c00188
ACS Catal. 2020, 10, 5236−5242

Authors

Jaeho Yoon − *Department of Materials Science and Engineering, Korea Advanced Institute of Science and Technology (KAIST), Daejeon 305-701, Republic of Korea*

Jinhyun Kim − *Department of Materials Science and Engineering, Korea Advanced Institute of Science and Technology (KAIST), Daejeon 305-701, Republic of Korea;* orcid.org/0000-0002-1616-1891

Florian Tieves − *Department of Biotechnology, Delft University of Technology, Delft 2629 HZ, The Netherlands*

Wuyuan Zhang − *Department of Biotechnology, Delft University of Technology, Delft 2629 HZ, The Netherlands;* orcid.org/0000-0002-3182-5107

Miguel Alcalde − *Department of Biocatalysis, Institute of Catalysis, CSIC, 28049 Madrid, Spain;* orcid.org/0000-0001-6780-7616

Complete contact information is available at: https://pubs.acs.org/10.1021/acscatal.0c00188

Notes

The authors declare no competing financial interest.

■ ACKNOWLEDGMENTS

This work was supported by the National Research Foundation (NRF) of Korea via the Creative Research Initiative Center (Grant No. NRF-2015R1A3A2066191) and the European Research Council (ERC Consolidator Grant No. 648026).

■ REFERENCES

(1) Bormann, S.; Gomez Baraibar, A.; Ni, Y.; Holtmann, D.; Hollmann, F. Specific Oxyfunctionalisations Catalysed by Peroxygenases: Opportunities, Challenges and Solutions. *Catal. Sci. Technol.* **2015**, *5*, 2038−2052.

(2) Karich, A.; Scheibner, K.; Ullrich, R.; Hofrichter, M. Exploring the Catalase Activity of Unspecific Peroxygenases and the Mechanism of Peroxide-dependent Heme Destruction. *J. Mol. Catal. B: Enzym.* **2016**, *134*, 238−246.

(3) Churakova, E.; Kluge, M.; Ullrich, R.; Arends, I.; Hofrichter, M.; Hollmann, F. Specific Photobiocatalytic Oxyfunctionalization Reactions. *Angew. Chem., Int. Ed.* **2011**, *50*, 10716−10719.

(4) Zhang, W.; Burek, B. O.; Fernández-Fueyo, E.; Alcalde, M.; Bloh, J. Z.; Hollmann, F. Selective Activation of C-H Bonds in a Cascade Process Combining Photochemistry and Biocatalysis. *Angew. Chem., Int. Ed.* **2017**, *56*, 15451−15455.

(5) Holtmann, D.; Hollmann, F. The Oxygen Dilemma: A Severe Challenge for the Application of Monooxygenases? *ChemBioChem* **2016**, *17*, 1391−1398.

(6) Valderrama, B.; Ayala, M.; Vazquez-Duhalt, R. Suicide Inactivation of Peroxidases and the Challenge of Engineering More Robust Enzymes. *Chem. Biol.* **2002**, *9*, 555−565.

(7) Freakley, S. J.; Kochius, S.; van Marwijk, J.; Fenner, C.; Lewis, R. J.; Baldenius, K.; Marais, S. S.; Opperman, D. J.; Harrison, S. T. L.; Alcalde, M.; Smit, M. S.; Hutchings, G. J. A Chemo-Enzymatic Oxidation Cascade to Activate C−H Bonds with *in situ* Generated H_2O_2. *Nat. Commun.* **2019**, *10*, 4178.

(8) Pesic, M.; Willot, S. J.-P.; Fernández-Fueyo, E.; Tieves, F.; Alcalde, M.; Hollmann, F. Multienzymatic *in situ* Hydrogen Peroxide Generation Cascade for Peroxygenase-catalysed Oxyfunctionalisation Reactions. *Z. Naturforsch., C: J. Biosci.* **2019**, *74*, 101.

(9) Willot, S. J. P.; Fernández-Fueyo, E.; Tieves, F.; Pesic, M.; Alcalde, M.; Arends, I. W. C. E.; Park, C. B.; Hollmann, F. Expanding the Spectrum of Light-Driven Peroxygenase Reactions. *ACS Catal.* **2019**, *9*, 890−894.

(10) van Schie, M. M. C. H.; Zhang, W.; Tieves, F.; Choi, D. S.; Park, C. B.; Burek, B. O.; Bloh, J. Z.; Arends, I. W. C. E.; Paul, C. E.; Alcalde, M.; Hollmann, F. Cascading g-C_3N_4 and Peroxygenases for Selective Oxyfunctionalization Reactions. *ACS Catal.* **2019**, *9*, 7409−7417.

(11) Horst, A. E. W.; Bormann, S.; Meyer, J.; Steinhagen, M.; Ludwig, R.; Drews, A.; Ansorge-Schumacher, M.; Holtmann, D. Electro-enzymatic Hydroxylation of Ethylbenzene by the Evolved Unspecific Peroxygenase of *Agrocybe aegerita*. *J. Mol. Catal. B: Enzym.* **2016**, *133*, S137−S142.

(12) Choi, D. S.; Ni, Y.; Fernández-Fueyo, E.; Lee, M.; Hollmann, F.; Park, C. B. Photoelectroenzymatic Oxyfunctionalization on Flavin-Hybridized Carbon Nanotube Electrode Platform. *ACS Catal.* **2017**, *7*, 1563−1567.

(13) Dagdeviren, C.; Shi, Y.; Joe, P.; Ghaffari, R.; Balooch, G.; Usgaonkar, K.; Gur, O.; Tran, P. L.; Crosby, J. R.; Meyer, M.; Su, Y.; Chad Webb, R.; Tedesco, A. S.; Slepian, M. J.; Huang, Y.; Rogers, J. A. Conformal Piezoelectric Systems for Clinical and Experimental Characterization of Soft Tissue Biomechanics. *Nat. Mater.* **2015**, *14*, 728.

(14) Ma, Y.; Liu, N.; Li, L.; Hu, X.; Zou, Z.; Wang, J.; Luo, S.; Gao, Y. A Highly Flexible and Sensitive Piezoresistive Sensor Based on MXene with Greatly Changed Interlayer Distances. *Nat. Commun.* **2017**, *8*, 1207.

(15) Han, M.; Wang, H.; Yang, Y.; Liang, C.; Bai, W.; Yan, Z.; Li, H.; Xue, Y.; Wang, X.; Akar, B.; Zhao, H.; Luan, H.; Lim, J.; Kandela, I.; Ameer, G. A.; Zhang, Y.; Huang, Y.; Rogers, J. A. Three-dimensional Piezoelectric Polymer Microsystems for Vibrational Energy Harvesting, Robotic Interfaces and Biomedical Implants. *Nat. Electron.* **2019**, *2*, 26−35.

(16) Mohapatra, H.; Kleiman, M.; Esser-Kahn, A. P. Mechanically Controlled Radical Polymerization Initiated by Ultrasound. *Nat. Chem.* **2017**, *9*, 135.

(17) Mushtaq, F.; Chen, X.; Torlakcik, H.; Steuer, C.; Hoop, M.; Siringil, E. C.; Marti, X.; Limburg, G.; Stipp, P.; Nelson, B. J.; Pané, S. Magnetoelectrically Driven Catalytic Degradation of Organics. *Adv. Mater.* **2019**, *31*, 1901378.

(18) Wang, M.; Zuo, Y.; Wang, J.; Wang, Y.; Shen, X.; Qiu, B.; Cai, L.; Zhou, F.; Lau, S. P.; Chai, Y. Remarkably Enhanced Hydrogen Generation of Organolead Halide Perovskites via Piezocatalysis and Photocatalysis. *Adv. Energy Mater.* **2019**, *9*, 1901801.

(19) Wu, J. M.; Chang, W. E.; Chang, Y. T.; Chang, C.-K. Piezo-Catalytic Effect on the Enhancement of the Ultra-High Degradation Activity in the Dark by Single- and Few-Layers MoS_2 Nanoflowers. *Adv. Mater.* **2016**, *28*, 3718−3725.

(20) Huang, H.; Tu, S.; Zeng, C.; Zhang, T.; Reshak, A. H.; Zhang, Y. Macroscopic Polarization Enhancement Promoting Photo- and Piezoelectric-Induced Charge Separation and Molecular Oxygen Activation. *Angew. Chem., Int. Ed.* **2017**, *56*, 11860−11864.

(21) Wang, M.; Wang, B.; Huang, F.; Lin, Z. Enabling PIEZOpotential in PIEZOelectric Semiconductors for Enhanced Catalytic Activities. *Angew. Chem., Int. Ed.* **2019**, *58*, 7526−7536.

(22) Bhachu, D. S.; Moniz, S. J. A.; Sathasivam, S.; Scanlon, D. O.; Walsh, A.; Bawaked, S. M.; Mokhtar, M.; Obaid, A. Y.; Parkin, I. P.; Tang, J.; Carmalt, C. J. Bismuth Oxyhalides: Synthesis, Structure and Photoelectrochemical Activity. *Chem. Sci.* **2016**, *7*, 4832−4841.

(23) Li, Y.; Hu, R.; Zhang, X.; Yin, Z.; Qiu, J.; Yang, Z.; Song, Z. Emergence of Photoluminescence Enhancement of Eu^{3+} Doped BiOCl Single-crystalline Nanosheets at Reduced Vertical Dimensions. *Nanoscale* **2018**, *10*, 4865−4871.

(24) Jiang, J.; Zhao, K.; Xiao, X.; Zhang, L. Synthesis and Facet-Dependent Photoreactivity of BiOCl Single-Crystalline Nanosheets. *J. Am. Chem. Soc.* **2012**, *134*, 4473−4476.

(25) Sun, L.; Xiang, L.; Zhao, X.; Jia, C.-J.; Yang, J.; Jin, Z.; Cheng, X.; Fan, W. Enhanced Visible-Light Photocatalytic Activity of BiOI/BiOCl Heterojunctions: Key Role of Crystal Facet Combination. *ACS Catal.* **2015**, *5*, 3540−3551.

(26) Shao, D.; Zhang, L.; Sun, S.; Wang, W. Oxygen Reduction Reaction for Generating H_2O_2 through a Piezo-Catalytic Process over Bismuth Oxychloride. *ChemSusChem* **2018**, *11*, 527−531.

(27) Guan, M.; Xiao, C.; Zhang, J.; Fan, S.; An, R.; Cheng, Q.; Xie, J.; Zhou, M.; Ye, B.; Xie, Y. Vacancy Associates Promoting Solar-Driven Photocatalytic Activity of Ultrathin Bismuth Oxychloride Nanosheets. *J. Am. Chem. Soc.* **2013**, *135*, 10411−10417.
(28) Wu, Y.; Yuan, B.; Li, M.; Zhang, W.-H.; Liu, Y.; Li, C. Well-defined BiOCl Colloidal Ultrathin Nanosheets: Synthesis, Characterization, and Application in Photocatalytic Aerobic Oxidation of Secondary Amines. *Chem. Sci.* **2015**, *6*, 1873−1878.
(29) Gao, S.; Sun, Z.; Liu, W.; Jiao, X.; Zu, X.; Hu, Q.; Sun, Y.; Yao, T.; Zhang, W.; Wei, S.; Xie, Y. Atomic Layer Confined Vacancies for Atomic-level Insights into Carbon Dioxide Electroreduction. *Nat. Commun.* **2017**, *8*, 14503.
(30) Wang, K.; Shao, D.; Zhang, L.; Zhou, Y.; Wang, H.; Wang, W. Efficient Piezo-Catalytic Hydrogen Peroxide Production from Water and Oxygen over Graphitic Carbon Nitride. *J. Mater. Chem. A* **2019**, *7*, 20383−20389.
(31) Wei, Y.; Zhang, Y.; Geng, W.; Su, H.; Long, M. Efficient Bifunctional Piezocatalysis of Au/$BiVO_4$ for Simultaneous Removal of 4-chlorophenol and Cr(Vi) in Water. *Appl. Catal., B* **2019**, *259*, 118084.
(32) Gao, E.; Wang, W. Role of Graphene on the Surface Chemical Reactions of $BiPO_4$−rGO with Low OH-related Defects. *Nanoscale* **2013**, *5*, 11248−11256.
(33) Kim, K.; Lee, S. H.; Choi, D. S.; Park, C. B. Photoactive Bismuth Vanadate Structure for Light-Triggered Dissociation of Alzheimer's *β*-Amyloid Aggregates. *Adv. Funct. Mater.* **2018**, *28*, 1802813.
(34) Ullrich, R.; Nüske, J.; Scheibner, K.; Spantzel, J.; Hofrichter, M. Novel Haloperoxidase from the Agaric Basidiomycete *Agrocybe aegerita* Oxidizes Aryl Alcohols and Aldehydes. *Appl. Environ. Microbiol.* **2004**, *70*, 4575.
(35) Molina-Espeja, P.; Garcia-Ruiz, E.; Gonzalez-Perez, D.; Ullrich, R.; Hofrichter, M.; Alcalde, M. Directed Evolution of Unspecific Peroxygenase from *Agrocybe aegerita*. *Appl. Environ. Microbiol.* **2014**, *80*, 3496.
(36) Aranda, E.; Marco-Urrea, E.; Caminal, G.; Arias, M. E.; García-Romera, I.; Guillén, F. Advanced Oxidation of Benzene, Toluene, Ethylbenzene and Xylene Isomers (BTEX) by *Trametes versicolor*. *J. Hazard. Mater.* **2010**, *181*, 181−186.
(37) Huang, M.; Wang, Z.; Hao, L.; Zhang, W. Theoretical Investigation on the Mechanism and Kinetics of OH Radical with Ethylbenzene. *Int. J. Quantum Chem.* **2011**, *111*, 3125−3134.
(38) Zhang, W.; Fernández-Fueyo, E.; Ni, Y.; van Schie, M.; Gacs, J.; Renirie, R.; Wever, R.; Mutti, F. G.; Rother, D.; Alcalde, M.; Hollmann, F. Selective Aerobic Oxidation Reactions Using a Combination of Photocatalytic Water Oxidation and Enzymatic Oxyfunctionalizations. *Nature Catalysis* **2018**, *1*, 55−62.
(39) Pryor, W. A. Oxy-Radicals and Related Species: Their Formation, Lifetimes, and Reactions. *Annu. Rev. Physiol.* **1986**, *48*, 657−667.
(40) Roots, R.; Okada, S. Estimation of Life Times and Diffusion Distances of Radicals Involved in X-Ray-Induced DNA Strand Breaks or Killing of Mammalian Cells. *Radiat. Res.* **1975**, *64*, 306−320.
(41) Puls, J.; Wilson, S. A.; Hölter, D. Degradation of Cellulose Acetate-Based Materials: A Review. *J. Polym. Environ.* **2011**, *19*, 152−165.
(42) Choi, D. S.; Lee, H. L.; Tieves, F.; Lee, Y. W.; Son, E. J.; Zhang, W.; Shin, B.; Hollmann, F.; Park, C. B. Bias-Free *in situ* H_2O_2 Generation in a Photovoltaic-Photoelectrochemical Tandem Cell for Biocatalytic Oxyfunctionalization. *ACS Catal.* **2019**, *9*, 10562−10566.
(43) Jin, C.; Liu, D.; Hu, J.; Wang, Y.; Zhang, Q.; Lv, L.; Zhuge, F. The Role of Microstructure in Piezocatalytic Degradation of Organic Dye Pollutants in Wastewater. *Nano Energy* **2019**, *59*, 372−379.
(44) Duan, J.; Kasper, D. L. Oxidative Depolymerization of Polysaccharides by Reactive Oxygen/Nitrogen Species. *Glycobiology* **2011**, *21*, 401−409.
(45) Danilczuk, M.; Perkowski, A. J.; Schlick, S. Ranking the Stability of Perfluorinated Membranes Used in Fuel Cells to Attack by Hydroxyl Radicals and the Effect of Ce(III): A Competitive Kinetics Approach Based on Spin Trapping ESR. *Macromolecules* **2010**, *43*, 3352−3358.
(46) Kim, J.; Lee, S. H.; Tieves, F.; Paul, C. E.; Hollmann, F.; Park, C. B. Nicotinamide Adenine Dinucleotide as a Photocatalyst. *Sci. Adv.* **2019**, *5*, No. eaax0501.
(47) Kim, J.; Lee, S. H.; Tieves, F.; Choi, D. S.; Hollmann, F.; Paul, C. E.; Park, C. B. Biocatalytic C = C Bond Reduction through Carbon Nanodot-Sensitized Regeneration of NADH Analogues. *Angew. Chem., Int. Ed.* **2018**, *57*, 13825−13828.
(48) Yoon, J.; Lee, S. H.; Tieves, F.; Rauch, M.; Hollmann, F.; Park, C. B. Light-Harvesting Dye−Alginate Hydrogel for Solar-Driven, Sustainable Biocatalysis of Asymmetric Hydrogenation. *ACS Sustainable Chem. Eng.* **2019**, *7*, 5632−5637.

https://dx.doi.org/10.1021/acscatal.0c00188
ACS Catal. 2020, 10, 5236−5242